RAPID COMMUNICATIONS

PHYSICAL REVIEW B VOLUME 47, NUMBER 22 1 JUNE 1993-II

Spin folding in the two-dimensional Heisenberg *kagomé* antiferromagnet

I. Ritchey
Low Temperature Physics Group, Cavendish Laboratory, Madingley Road, Cambridge CB3 0HE, United Kingdom

P. Chandra
NEC Research Institute, 4 Independence Way, Princeton, New Jersey 08540

P. Coleman
Serin Physics Laboratory, Rutgers University, P. O. Box 849, Piscataway, New Jersey 08854
(Received 7 July 1992)

Spin-folding modes in the two-dimensional Heisenberg *kagomé* antiferromagnet favor coplanar spin configurations with three-spin tensor order and *non-Abelian* homotopy. With weak *xy* anisotropy, binding of the associated disclinations yields a coplanar state whose spin configuration depends on the order of pairing. The resulting metastable states exhibits a broad distribution of order parameters. Supporting numerical studies are presented and the related system $SrCr_{8-x}Ga_{4+x}O_{19}$ is discussed.

The spin-$\frac{3}{2}$ magnetoplumbite $SrCr_{8-x}Ga_{4+x}O_{19}$ (SCGO) is an enigmatic spin glass: the nonlinear susceptibility[1] (χ_3) indicates $T_g=3.5$ K $\sim\Theta_{CW}/100$, where T_g and Θ_{CW} are the glass transition and Curie-Weiss $[\Theta_{CW}=\frac{4}{3}JS(S+1)]$ temperatures, respectively, and the low-temperature specific heat[1] is *quadratic* ($c_v\sim T^2$); by contrast, the conventional spin glass[2] has $T_g\sim\Theta_{CW}$ and $c_v\sim T$. The magnetic properties of SCGO are attributed to planes of antiferromagnetically coupled Cr^{3+} atoms on a *kagomé* lattice; each chromium is associated with an isotropic $S=\frac{3}{2}$ moment.[3] The two-dimensional (2D) nature of the frozen spin correlations has been confirmed by quasielastic neutron studies.[4] Inelastic measurements indicate strong moment fluctuations at $T<T_g$ and a frequency-independent cross section at low-energy scales ($\omega<\omega_0=c/\xi$) consistent with a Goldstone mode in the spin channel.[4] Conventional spin glass behavior is associated with the formation of low-energy domain walls in a *randomly* frustrated magnet;[5] for the Heisenberg case, renormalization treatments[2] yield a lower critical dimension $d_l\geq 4$. Motivated by the SCGO experiments, we propose a disorder-free mechanism for quasi-2D glassy behavior; it relies on the unique homotopy associated with spin nematic order[6-8] that admits *non-Abelian* point disclinations.

The simplest magnetic model of SCGO is the 2D nearest-neighbor Heisenberg antiferromagnet (AFM) $H=J\sum_{(i,j)}\mathbf{S}_i\cdot\mathbf{S}_j$ on a *kagomé* lattice (Fig. 1); classically, the constraint on each plaquette $\sum_{(i\in\Delta)}\mathbf{S}_i=0$ fails to define a unique ground state.[9,10] Like its triangular counterpart, the *kagomé* magnet admits a coplanar ground-ground-state spin configuration; however, its unique geometry also permits continuous *spin folding* zero-energy modes that preserve the 120° spin orientation through the introduction of "spin facets." "Open" spin folds [Fig. 1(a)] traversing the entire lattice are present in a state of *uniform* spin chirality; a configuration of *staggered* chirality has "closed" folds [Fig. 1(b)], where the spins within the facet edges can rotate about the common axis of their perimeter spins with no energy cost.

In a degenerate manifold, fluctuations select the states with maximal flexibility;[11-13] here it is the coplanar configurations that minimize the associated free energy. Physically, a fold through an angle ϕ ($\phi\neq\pi$) "stiffens" all intersecting ones increasing their frequencies; the *kagomé* magnet thus acquires a geometric spin rigidity similar to that of a paper Origami structure. In a coplanar configuration ($\phi=\pi$), the energy cost of infinite π-folds is negligible, but their creation involves overcoming extensive energy barriers. The cooling of the *kagomé* magnet thus yields a locally coplanar configuration with a discrete set of 120° spin orientations. In this paper we propose that in any such process, this "typical" state is selected in an essentially *unbiased* way; at lower tempera-

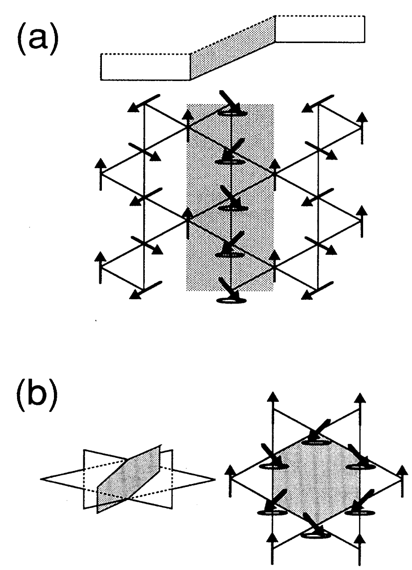

FIG. 1. (a) Open and (b) closed folds in the states of uniform and staggered spin chirality, respectively. Spin orientations in the diagram denote orientations in the internal *spin space.* A weak *xy* anisotropy aligns the *z* axis of the internal spin space with the physical *z* axis.

tures global annealing is inhibited by the necessary creation of infinite π-folds.

In the "typical" coplanar configuration there are *nematic* spin correlations with planar threefold symmetry; the corresponding tensor order parameters,[7] described by three unit vectors $\hat{e}_\lambda$ ($\lambda=1,3$), where $\sum \hat{e}_\lambda=0$, are

$$\langle S^\alpha(x)S^\beta(y)S^\gamma(z)\rangle = t(x,y,z) f_{\alpha\beta\gamma}\hat{e}_1^\alpha \hat{e}_2^\beta \hat{e}_3^\gamma \ ,$$
$$\langle S^\alpha(x)S^\beta(y)\rangle - \tfrac{1}{3}\delta^{\alpha\beta}\langle \mathbf{S}(x)\cdot\mathbf{S}(y)\rangle = q(x-y)(\hat{n}^\alpha\hat{n}^\beta - \tfrac{1}{3}\delta^{\alpha\beta}) \ , \tag{1}$$

where $\hat{n}$ is the director normal to the spin plane and $f_{\alpha\beta\gamma}=|\epsilon_{\alpha\beta\gamma}|$ is the fully symmetric tensor. The order parameters in (1) have *discrete* hexagonal C_{3h} symmetry; the homotopy associated with their allowed point defects, $\Pi_1(R)=D_{3h}$, is *non-Abelian,* where D_{3h} is the double-group[14] generated by the elements $\{g_\lambda\}=\{i\hat{e}_\lambda\cdot\boldsymbol{\sigma}\}$. These "point disclinations" correspond to π rotations of $\hat{n}$ about the $\hat{e}_\lambda$, and the 180° line singularities linking two identical point defects are naturally identified with the π-folds discussed above. Unlike their conventional $U(1)$ counterparts, non-Abelian defects affect the *local* spin state; their presence leads to a large ground-state degeneracy and the possibility of glassy behavior.

Within Gaussian spin-wave theory, we have calculated the energy barrier associated with the creation of a spin fold. The addition of a spin facet at an angle ϕ to the surrounding spin plane modifies the magnon pairing field $\Delta\to e^{2i\phi}\Delta$ within the facet; π-folds are thus invisible to spin waves and all coplanar configurations exhibit an identical flat band of Gaussian zero modes. ϕ-fold angles ($\phi<\pi$) constitute a *degenerate* perturbation within this manifold; for small ϕ all intersecting folds have an increased frequency $\delta\omega_n\sim JS|\delta\phi|$. The resulting energy barrier appears in the simple illustrative example of applied uniform curvature; for the planar configuration with uniform spin chirality a uniform phase gradient $\phi(x)=x\phi$ is introduced to the magnon pairing field along the a crystal axis. By projecting the Hamiltonian into the low-energy subspace of original Gaussian zero modes, the leading-order perturbation in the zero-point energy of this band is

$$V(\phi)=\eta L|\sin\phi| \ , \tag{2}$$

where $\eta=0.14JS$ and L is the number of spins per fold line. At finite temperatures,

$$V(\phi)\sim TL\ln[2\sinh|\beta\eta\sin\phi|] \tag{3}$$

indicating an analogous entropic selection of coplanarity, recently confirmed by numerical studies;[15] (2) and (3) are valid for $\sin^2\phi>\sin^2\phi_0$, where $\phi_0^C\sim\sqrt{T/J}$ and $\phi_0^{QM}\sim 1/S^{1/3}$ are the classical and quantum mechanical root-mean-squared fluctuations in ϕ, respectively. The height of the fluctuation-selected potential barrier (per length of fold) is $V_0\sim\eta JS$ and $V_0\sim T\ln(\eta JS/T)$ in the quantum ($S\ll JS^2/T$) and classical ($S\gg JS^2/T$) regimes, respectively.

Each configuration within this coplanar manifold can be identified with a ground state of the three-state Potts model on the same lattice;[4] there are W^N states where $W=1.1833\ldots$ and N is the number of sites.[16] Loops of alternating spin orientations ($abab\ldots$) are identified in all configurations; numerical studies reveal a power-law probability distribution, $p(L)\sim L^{-\zeta}$ with $\zeta\sim1.34(\pm0.02)$, for the loop length passing through any given site in a *typical* coplanar state.[17,18] Since the associated tunneling barrier has height $V\sim L$, the distribution of barrier heights in this manifold is also self-similar $[P(V)\sim V^{-\zeta}]$. Each triangular plaquette is characterized by its chirality $\tau=(1/3\sin120°)|\sum_{j,k}\mathbf{S}_j\times\mathbf{S}_k|$, where cross products are evaluated in a clockwise-sense around plaquettes; $\tau_s=\tau_\Delta-\tau_\nabla$, is the chirality difference on opposite triangular sublattices, the chiral analogue of the staggered magnetization. The generalized Edwards-Anderson order parameter, $\chi_{ch}=(1/N(\sum_i\tau_S)^2$, measures the overlap of a given state with one of uniform staggered spin chirality. This intensive quantity has an exponential probability distribution[18] with a finite variance, $P(\chi_{ch})\sim e^{-\chi_{ch}/\chi_0}$ with $\chi_0\sim3.29$.

The development of a smooth, locally coplanar configuration in the Heisenberg *kagomé* spin system demands the absence of topological defects that are stable in any noncollinear 2D Heisenberg antiferromagnet.[19,14] Here spin-wave interactions drive the spin stiffness to zero at long length scales;[20] the resulting finite spin correlation length implies that a small density of these defects will always exist in the low-temperature phase. Thus the development of the coplanar spin state is a crossover from a high-temperature defect-rich regime to a low-temperature phase with an exponentially small density of defects.[19,18] In the real system infinitesmal xy anisotropy is strongly relevant;[21] it provides a new length scale l_0 beyond which out-of-plane fluctuations develop a gap and further renormalization of the stiffness is suppressed. Exponentially small amounts of xy anisotropy are thus sufficient to convert the crossover to a true topological phase transition; we will thus include such a term in our discussion.

The simplest long-wavelength action with an $SU(2)\times C_{3h}$ symmetry

$$S=\frac{\gamma}{12T}\int d^2x\,\mathrm{Tr}\{\Lambda\nabla\mathcal{G}^\dagger\nabla\mathcal{G}+\epsilon\underline{\sigma}^3\mathcal{G}^\dagger\underline{\sigma}^3\mathcal{G}\} \ ,$$
$$\Lambda_{ab}=\underline{1}+f_{abc}\hat{e}_c\cdot\underline{\boldsymbol{\sigma}} \ , \tag{4}$$

where γ is the spin-wave stiffness; the order parameter $\mathcal{G}(x)=g\otimes\underline{1}$, an external product of an SU(2) and a unit 3×3 matrix, is an $S=\frac{3}{2}$ representation of the rotation group. A small xy anisotropy ϵ about an axis perpendicular to the triad $\hat{e}_\lambda$ has been introduced; ϵ could originate from site or bond anisotropy in the original model, or from an applied external field. The discrete non-Abelian symmetry appears as a right-invariance of the order parameter $\mathcal{G}\to\mathcal{G}_{g\lambda}$. For $\epsilon=0$, there is a rapid crossover[19,18] at $T^*\sim\gamma$ from a defect-dominated regime ($\rho_D\sim1$) to one of exponentially small defect density $\rho_D\sim e^{-(T^*/T)^2}$; for $T<T^*$, spin waves[20] determine the spin correlation length $\xi\sim ae^{4\pi\gamma/T}$, where a is the lattice spacing.

A finite anisotropy ($\epsilon\neq0$) yields a length scale $l_0\sim a/\sqrt{\epsilon}$ ($l_0\to a$ for $\epsilon>1$); for distances $l>l_0$ the system is effectively an xy magnet. If $l_0<\xi$, this anisotropy results in the *linear* confinement of the 180° point defects; they bind in pairs to generate 120° point disclinations thus avoiding anisotropic energy costs ($g_a g_b = h_{120}$ for $a \neq b$, where $h_{120} = e^{i(\pi/3)\sigma_3}$). Furthermore, if $l_0 < \xi(T^*)$, i.e., $\epsilon > \epsilon_0 = e^{-8\pi\gamma/T^*} \ll 1$, 120° defects will bind at a Kosterlitz-Thouless (KT) temperature $T_{\rm KT} \sim T^*$. Figure 2 illustrates the three important regimes of this model: (i) $T > T_\pi$ ($\xi < l_0$) all defects are free; (ii) $T_\pi > T > T_{\rm KT}$ ($\xi > l_0$) free 120° defects (bound pairs of 180° disclinations); and (iii) $T < T_{\rm KT}$ ($\xi \to \infty$) all defects are bound. In the limit $\epsilon \to \epsilon_0, T_\pi \sim T_{\rm KT}$; T_π is always a crossover due to the possible exchange of 180° disclinations by two 120° defects. For $\epsilon \to 0$ the transition temperature scales weakly with anisotropy $[T \sim 1/\ln(1/\epsilon)]$, and thus the phase boundary has a sharp downward turn to the origin in the pure Heisenberg limit ($\epsilon = 0$).

The realization of Fig. 2 requires the entropic selection of the coplanar manifold; this must occur at a temperature where its free energy is lower than that of its rival ordered states. Higher-order fluctuations tend to break this coplanar degeneracy, favoring an ordered configuration with an energy $-\Delta E \sim -J$ (per site) *relative* to that of the typical state.[22] The latter has an entropy $\ln W$; at $T = T_{\rm KT} \sim \pi\gamma/18$ it is selected if

$$T_{\rm KT} > T_0 = \Delta E / \ln W \ . \tag{5}$$

For $T < T_0$, the typical state is thermodynamically unstable to the magnet; however, infinite π-folds inhibit global annealing, thus ensuring the *kinetic* stability of the typical configuration. Higher-order quantum fluctuations generate a chirality coupling $E = -\alpha \sum_{\{\Delta,\nabla\}} \langle \tau_\Delta \cdot \tau_\nabla \rangle \propto \chi_{\rm ch}$

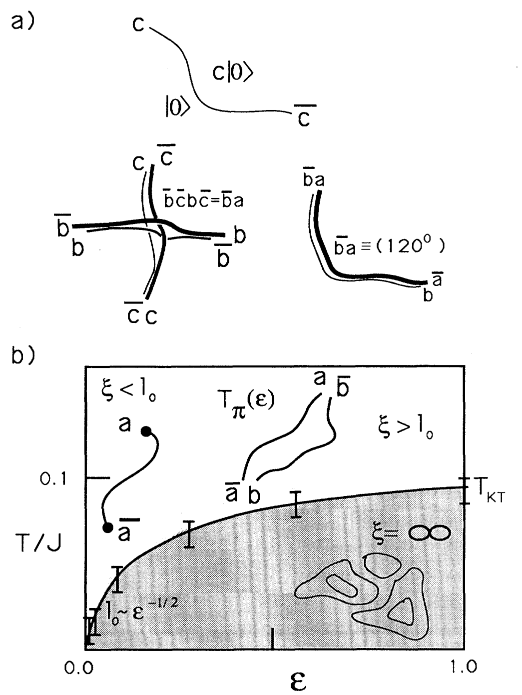

FIG. 2. (a) Formation of a 120° defect from a combination of π disclinations that nominally cancel one another, illustrating the dependence of configuration on the order in which disclination pairs are separated to infinity. (b) Phase diagram for the anisotropic *kagomé* antiferromagnet; numerical data points for the Kosterlitz-Thouless temperature $T_{\rm KT}$ as a function of anisotropy (ϵ) are superimposed.

between neighboring plaquettes; the energy per site thus acquires an exponential distribution similar to that of the chiral susceptibility $P(E) \sim P(-\alpha\chi_{\rm ch})$. Since χ_3 scales with the intervalley energy fluctuations ($\chi_3 \sim -N\overline{E^2}$), the freezing of the typical state results in a negative divergence of the nonlinear susceptibility.

Several features of the proposed binding transition distinguish it from the conventional Kosterlitz-Thouless[23] (KT) case. First, it is a true second-order phase transition; the three-state Potts order breaks the lattice symmetry, resulting in a specific heat *divergence.* Next, the gradient field associated with a 120° defect is $\alpha = \frac{1}{3}$ times that of a 360° vortex; the attractive energy between two vortices, and thus $T_{\rm KT}$, is reduced by a factor $q^2 = \frac{1}{9}$. The standard KT estimate[23] then yields $T_{\rm KT} \approx q^2 \pi\gamma/2 = \pi\gamma/18$. An upper limit for γ in the extreme xy limit of the *kagomé* magnet is $\gamma = JS^2/2$; the resulting $T_{\rm KT} = JS^2\pi/36 \approx T_{\rm CW}/48$ demonstrates that an essential consequence of 120° defect binding is the large reduction in the transition temperature. Finally, we also note that the ground-state manifold has a "memory" of past defect motion. As in the KT problem, transitions between different "ground states" occur through the separation to infinity of two bound defects; there, the final state does not depend on the details of the process, and configurations are characterized by two winding numbers. This simple classification scheme is not possible for non-Abelian disclinations where the resulting configurations are determined by the detailed braiding of the textures formed by the defect paths (see Fig. 2).[24,14]

To test these ideas, we have performed Monte Carlo simulations on the classical Heisenberg *kagomé* antiferromagnet with a weak bond xy anisotropy $\delta J_z = -\epsilon J$ which is easy to implement within a heat bath algorithm. The anisotropy was varied in the range $0.01 < \epsilon < 1.0$, to avoid the first-order phase transition into a ferromagnet at $\epsilon = 1.5$. Arrays of 108, 432, and 864 spins were sequentially cooled from a random configuration, with 1.25×10^6 spin flips per site per temperature. Thermal averages were also performed over short periods of 1.25×10^3 updates; they provided 10^3 approximately independent samples where the distribution of thermodynamic variables was examined. The KT transition was identified from a jump in the spin-wave stiffness (Fig. 3) which vanishes for $\epsilon = 0$; numerical values of $T_{\rm KT}(\epsilon)$ are indicated in Fig. 2. For $\epsilon \neq 0, C_v$ displays a divergence at the transition (Fig. 3). As in the $J_1 - J_2$ Heisenberg problem,[13,18] the lattice-symmetry breaking crossover is transformed to a true phase transition by xy anisotropy ($\epsilon \neq 0$); extrapolation of $T_{\rm KT}$ to $\epsilon = 0$ yields a crossover temperature $T^*(0) \sim 0.01$ J.

The antisymmetric part of the nematic spin susceptibility $\chi_{\rm ch}$ remains finite at low temperatures indicating the *absence* of $\sqrt{3} \times \sqrt{3}$ ordering. By contrast, $\overline{\chi^2_{\rm ch}}$ jumps rapidly at a temperature $T \lesssim T^*$, suggesting the development of glassy behavior. At $T_{\rm KT}$, only the long folds drop out of equilibrium, and at lower temperature, single star transitions still persist. In our simulations, single star flips freeze out at a temperature $\sim T_{\rm KT}/2$, where a cusp in $\chi_{\rm ch}$ is observed. Longer simulations are required

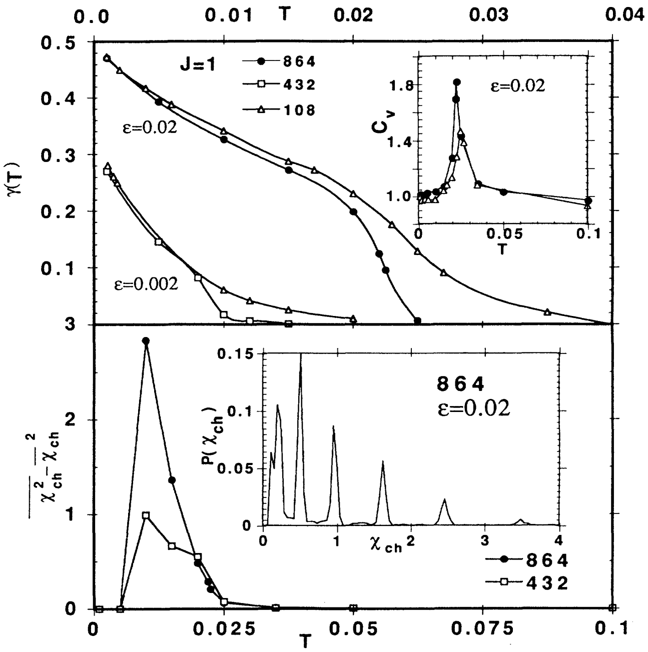

FIG. 3. (top) Spin stiffness about z axis for 108, 432, and 864 spins at $\epsilon=0.002$ and 0.02 (inset: C_v for $\epsilon=0.02$). (bottom) Divergence in $\overline{\chi_{\rm ch}^2}$ for $\epsilon=0.02$, 4.32, and 864 spins (inset: distribution of $\chi_{\rm ch}$ for $\epsilon=0.02$ and $T/J=0.010$ for 864 spins).

to examine dynamical aspects associated with the freezing of longer folds. Figure 3 displays the distribution of $\chi_{\rm ch}$ at low temperatures where single star flips are still dynamically equilibrated, displaying a distribution similar to the typical Potts state on the same lattice.

These results clearly indicate that the low-temperature phase of the anisotropic *kagomé* system is *not* a conventional magnet. A careful study of the relaxation time scales must be performed to probe the glassy nature of the low-temperature phase. In particular, details of the noise spectrum would provide information about the nature of the barriers, distinguishing between droplet and hierarchical glassiness.[25] Experimentally, many of the SCGO measurements can be reconciled within such a quasi-two-dimensional picture. Within any given coplanar state, the *kagomé* spin system has a frozen moment, and thus a Goldstone mode in the spin channel, consistent with a T^2 specific heat and a flat inelastic neutron scattering cross section. Future susceptibility and neutron measurements on both single crystals and epitaxial films of SCGO will provide further evidence of its 2D nature. A definite test of our theory is the field dependence of the glass transition temperature (T_g): In a conventional spin glass an external field suppresses T_g; by contrast, the topological freezing picture predicts an *enhancement* of the glass temperature as the anisotropy is increased with applied field.

In conclusion, we have presented a model for glassy behavior in the *absence* of extrinsic disorder; here the glass transition is associated with the binding of *non-Abelian* textures. Provisional numerical studies support this picture, and specific application to SCGO may reconcile the absence of several conventional spin glass features with the observed divergence of the nonlinear susceptibility.

It is a pleasure to acknowledge discussions with G. Aeppli, J. Banavar, C. Broholm, D. Huse, G. Lonzarich, S. Nagel, A. Ramirez, N. Read, S. Sachdev, W. Saslow, A. Schofield, and P. Young. I. Ritchey thanks Rutgers University and NEC Research Institute for their hospitality. Numerical work was performed on an NEC SX-3 at the HNSX Supercomputer Center (Woodlands, Texas); we are grateful to D. Branch for her assistance there. P. Coleman acknowledges financial support from NSF Grant No. DMR-89-13692 and the Sloan Foundation.

[1]A. P. Ramirez, G. P. Espinosa, and A. S. Cooper, Phys. Rev. Lett. **64**, 2070 (1990).
[2]K. Binder and A. P. Young, Rev. Mod. Phys. **58**, 801 (1986).
[3]X. Obradors, A. Labarta, A. Isalgue, J. Tejada, J. Rodriguez, and M. Pernet, Solid State Commun. **65**, 189 (1988).
[4]C. Broholm, G. Aeppli, G. P. Espinosa, and A. S. Cooper, Phys. Rev. Lett. **65**, 3173 (1990); C. Broholm, G. Aeppli, G. P. Espinosa, and A. S. Cooper, J. Appl. Phys. **69**, 4968 (1990).
[5]G. Toulouse, Phys. Rep. **49**, 267 (1979).
[6]I. E. Dzyaloshinski, Zh. Eskp. Teor. Fiz. **32**, 1547 (1957) [Sov. Phys. JETP **5**, 1259 (1957)]; A. F. Andreev and I. A. Grishchuk, *ibid.* **87**, 467 (1984) [**60**, 267 (1984)].
[7]V. I. Marchencko, Pis'ma Zh. Eskp. Teor. Fiz. **47**, 357 (1988) [JETP Lett. **47**, 428 (1988)]; L. P. Gorkov, Europhys. Lett. **16**, 301 (1991).
[8]P. Chandra and P. Coleman, Phys. Rev. Lett. **66**, 100 (1991); P. Chandra, P. Coleman, and I. Ritchey, Int. J. Mod. Phys. **5**, 17 (1991).
[9]V. Elser, Phys. Rev. Lett. **62**, 2405 (1989); C. Zeng and V. Elser, Phys. Rev. B **42**, 8436 (1990).
[10]J. B. Marston and C. Zeng, J. Appl. Phys. **69**, 5962 (1991); T. C. Hsu and A. J. Schofield, J. Phys. Condens. Matter **3**, 8067 (1991).
[11]J. Villain, J. Phys. (Paris) **38**, 26 (1977); J. Villain, R. Bidaux, J. P. Carton, and R. Conte, *ibid.* **41**, 1263 (1980).
[12]C. L. Henley, Phys. Rev. Lett. **62**, 2056 (1989).
[13]P. Chandra, P. Coleman, and A. I. Larkin, Phys. Rev. Lett. **64**, 88 (1990).
[14]N. D. Mermin, Rev. Mod. Phys. **51**, 591 (1979).
[15]J. T. Chalker, P. C. W. Holdsworth, and E. F. Shendar, Phys. Rev. Lett. **68**, 855 (1992).
[16]R. J. Baxter, J. Math. Phys. **11**, 784 (1970).
[17]D. A. Huse and A. Rutenberg, Phys. Rev. B **45**, 7536 (1992).
[18]I. Ritchey, Trinity College Fellowship Dissertation, 1991; P. Chandra, P. Coleman, and I. Ritchey, J. Phys. I (France) **3**, 591 (1993).
[19]H. Kawamura and S. Miyashita, J. Phys. Soc. Jpn. **53**, 9 (1984).
[20]A. M. Polyakov, Phys. Lett. **59B**, 97 (1975).
[21]V. L. Pokrovsky, Adv. Phys. **28**, 595 (1979).
[22]S. Sachdev, Phys. Rev. B **45**, 12 377 (1992); A. J. Berlinsky, C. Kallin, and A. B. Harris, Phys. Rev. B **45**, 2899 (1992); N. Read (unpublished); E. P. Chan and C. L. Henley, Bull. Am. Phys. Soc. **37**, 603 (1992).
[23]J. M. Kosterlitz and D. J. Thouless, J. Phys. C **6**, 1181 (1973).
[24]V. Poénaru and G. Toulouse, J. Phys. (Paris) **8**, 887 (1977).
[25]M. B. Weissman, N. E. Israeloff, and G. B. Alers, J. Magn. Magn. Mater., **114**, 87 (1992).